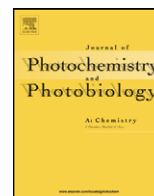




Contents lists available at ScienceDirect

Journal of Photochemistry and Photobiology A: Chemistry

journal homepage: www.elsevier.com/locate/jphotochem

Subject Index of Volume 203

Acetaldehyde oxidation

Physico-chemical, photo-catalytic and O₂-adsorption properties of TiO₂ nanotubes coated with gold nanoparticles, 24

Acetylperoxyl radical

Laser flash photolysis of new water-soluble peroxyl radical precursor, 13

4-Acetyl-4-phenylpiperidine hydrochloride

Laser flash photolysis of new water-soluble peroxyl radical precursor, 13

Acid Orange 7

Correlation of oxidative and reductive dye bleaching on TiO₂ photocatalyst films, 119

Acridinium ester

Synthesis and properties of novel chemiluminescent biological probes: 2- and 3-(2-Succinimidyloxycarbonyl)phenyl acridinium esters, 72

Adiabatic photoisomerization

Solvent-driven adiabatic *trans*-to-*cis* photoisomerization of 4-styrylquinoline, 100

Anthracene

Anthracene labeled pyridine amides: A class of prototype PET sensors towards monocarboxylic acid, 40

Construction of light-harvesting reverse micelles in nanoscopic dimensions, 56

Antimicrobial

Photochemistry of nitro-substituted (*E*)-2-azachalcones with theoretical calculations and biological activities, 85

Antioxidant

Photochemistry of nitro-substituted (*E*)-2-azachalcones with theoretical calculations and biological activities, 85

Atomic force microscopy

Dependence of photoinduced surface friction force variation on UV intensity and atmosphere in polycrystalline TiO₂ thin films, 155

Aza-aromatics

The phosphorescent triplet states of aza-aromatics and their protonated cations in rigid solutions of ethanol and 1-butyl-3-methylimidazolium hexafluorophosphate, 18

Benzotriazole

Thioxanthone-benzotriazole: Initiator and stabilizer properties in one component, 81

Butylparaben

Photodegradation of butylparaben in aqueous solutions by 254 nm irradiation, 131

Cadmium sulfide

Photocatalytic growth of CdS, PbS, and Cu_xS nanoparticles on the nanocrystalline TiO₂ films, 137

Cationic oxazolyfulgimides

Photochromic properties of cationic oxazolyfulgimides in hydroxylic media, 161

Charge separation

Photoinduced single- and double-electron transfer in a photosynthetic model consisting of one-acceptor with four equally linked donors (D₄-A), 216

Chemiluminescence

Synthesis and properties of novel chemiluminescent biological probes: 2- and 3-(2-Succinimidyloxycarbonyl)phenyl acridinium esters, 72

Chemiluminescence immunoassay

Synthesis and properties of novel chemiluminescent biological probes: 2- and 3-(2-Succinimidyloxycarbonyl)phenyl acridinium esters, 72

α -Cleavage

Laser flash photolysis of new water-soluble peroxyl radical precursor, 13

Complex

A water-soluble two-photon photopolymerization initiation system: Methylated- β -cyclodextrin complex of xanthene dye/aryliodonium salt, 211

Complexation

Complexation of Mg-tetrabenzoporphyrin with pyridine enhances singlet oxygen generation and affects its partitioning into apolar microenvironments, 7

Copper sulfide

Photocatalytic growth of CdS, PbS, and Cu_xS nanoparticles on the nanocrystalline TiO₂ films, 137

Correlation

Correlation of oxidative and reductive dye bleaching on TiO₂ photocatalyst films, 119

Cyclodextrin

A water-soluble two-photon photopolymerization initiation system: Methylated- β -cyclodextrin complex of xanthene dye/aryliodonium salt, 211

Degradation

Effect of Fe³⁺ ion doping to TiO₂ on the photocatalytic degradation of Malachite Green dye under UV and vis-irradiation, 64

Degussa P25

Sol-gel modified TiO₂ powder films for high performance dye-sensitized solar cells, 192

Diarylethylene

Solvent-driven adiabatic *trans*-to-*cis* photoisomerization of 4-styrylquinoline, 100

Diphenyliodonium salt

A water-soluble two-photon photopolymerization initiation system: Methylated- β -cyclodextrin complex of xanthene dye/aryliodonium salt, 211

DNA cleavage

Efficient photocleavage of DNA utilizing water soluble riboflavin/naphthaleneacetate substituted fullerene complex, 105

DODAB

Characterization of mixed DODAB/monoolein aggregates using Nile Red as a solvatochromic and anisotropy fluorescent probe, 32

Donor-acceptor π -conjugated fluorophores

Photovoltaic performance of dye-sensitized solar cells based on a series of new-type donor-acceptor π -conjugated sensitizer, benzofuro [2,3-*c*]oxazolo[4,5-*a*]carbazole fluorescent dyes, 177

- Dye-sensitized solar cells
- Dye-sensitized solar cells containing polymer film with honey-comb like morphology, 151
 - Photovoltaic performance of dye-sensitized solar cells based on a series of new-type donor-acceptor π -conjugated sensitizer, benzofuro[2,3-*c*]oxazolo[4,5-*a*]carbazole fluorescent dyes, 177
 - Sol-gel modified TiO₂ powder films for high performance dye-sensitized solar cells, 192
- Electrochemistry
- Intramolecular interactions and photoinduced electron transfer in isoalloxazine-naphthalene bichromophores, 166
- Electron affinity
- A density functional theory study on photophysical properties of red light-emitting materials: Meso-substituted porphyrins, 92
- Electron paramagnetic resonance
- The phosphorescent triplet states of aza-aromatics and their protonated cations in rigid solutions of ethanol and 1-butyl-3-methylimidazolium hexafluorophosphate, 18
- Electron transfer
- Intramolecular interactions and photoinduced electron transfer in isoalloxazine-naphthalene bichromophores, 166
 - Photoinduced single- and double-electron transfer in a photosynthetic model consisting of one-acceptor with four equally linked donors (D₄-A), 216
- Estrogenic compounds
- Photodegradation of butylparaben in aqueous solutions by 254 nm irradiation, 131
- Extra virgin olive oil
- Photodegradation of phytosanitary molecules present in virgin olive oil, 1
- Fe³⁺-doping
- Effect of Fe³⁺ ion doping to TiO₂ on the photocatalytic degradation of Malachite Green dye under UV and vis-irradiation, 64
- Flavine
- Intramolecular interactions and photoinduced electron transfer in isoalloxazine-naphthalene bichromophores, 166
- Fluorescence
- Photovoltaic performance of dye-sensitized solar cells based on a series of new-type donor-acceptor π -conjugated sensitizer, benzofuro[2,3-*c*]oxazolo[4,5-*a*]carbazole fluorescent dyes, 177
 - Solvent and central metal effects on the photophysical and photochemical properties of peripherally tetra mercaptopyridine substituted metallophthalocyanines, 204
- Formulant
- Photosensitizing properties of formulation adjuvants, 186
- Friction
- Dependence of photoinduced surface friction force variation on UV intensity and atmosphere in polycrystalline TiO₂ thin films, 155
- Fullerene
- Efficient photocleavage of DNA utilizing water soluble riboflavin/naphthaleneacetate substituted fullerene complex, 105
- Gel electrolyte
- Dye-sensitized solar cells containing polymer film with honey-comb like morphology, 151
- Gold co-catalyst
- Physico-chemical, photo-catalytic and O₂-adsorption properties of TiO₂ nanotubes coated with gold nanoparticles, 24
- Heterocycles
- Photovoltaic performance of dye-sensitized solar cells based on a series of new-type donor-acceptor π -conjugated sensitizer, benzofuro[2,3-*c*]oxazolo[4,5-*a*]carbazole fluorescent dyes, 177
- Hydration
- Characterization of mixed DODAB/monoolein aggregates using Nile Red as a solvatochromic and anisotropy fluorescent probe, 32
- Hydrogen production
- Photoactive component-loaded Nafion film as a platform of hydrogen generation: Alternative utilization of a classical sensitizing system, 112
- Hydroxylic media
- Photochromic properties of cationic oxazolylfulgimides in hydroxylic media, 161
- Initiator
- A water-soluble two-photon photopolymerization initiation system: Methylated- β -cyclodextrin complex of xanthene dye/aryliodonium salt, 211
- Intrinsic emission
- Intrinsic luminescence properties of ionic liquid crystals based on PAMAM and PPI dendrimers, 50
- Ionic liquid
- The phosphorescent triplet states of aza-aromatics and their protonated cations in rigid solutions of ethanol and 1-butyl-3-methylimidazolium hexafluorophosphate, 18
- Ionization potential
- A density functional theory study on photophysical properties of red light-emitting materials: Meso-substituted porphyrins, 92
- Ishihara ST-01
- Sol-gel modified TiO₂ powder films for high performance dye-sensitized solar cells, 192
- Kinetics parameters
- Photodegradation of phytosanitary molecules present in virgin olive oil, 1
- Laser flash photolysis
- Laser flash photolysis of new water-soluble peroxy radical precursor, 13
- Lead sulfide
- Photocatalytic growth of CdS, PbS, and Cu_xS nanoparticles on the nanocrystalline TiO₂ films, 137
- Ligand
- Complexation of Mg-tetrabenzoporphyrin with pyridine enhances singlet oxygen generation and affects its partitioning into apolar microenvironments, 7
- Light-harvesting reverse micelle
- Construction of light-harvesting reverse micelles in nanoscopic dimensions, 56
- Liposomes
- Complexation of Mg-tetrabenzoporphyrin with pyridine enhances singlet oxygen generation and affects its partitioning into apolar microenvironments, 7
- Luminescent liquid crystal
- Intrinsic luminescence properties of ionic liquid crystals based on PAMAM and PPI dendrimers, 50
- Macrocycles
- Intramolecular interactions and photoinduced electron transfer in isoalloxazine-naphthalene bichromophores, 166
- Membrane
- Dye-sensitized solar cells containing polymer film with honey-comb like morphology, 151
- 2-Mercaptopyridine
- Solvent and central metal effects on the photophysical and photochemical properties of peripherally tetra mercaptopyridine substituted metallophthalocyanines, 204
- Metallophthalocyanine
- Solvent and central metal effects on the photophysical and photochemical properties of peripherally tetra mercaptopyridine substituted metallophthalocyanines, 204
- Methylene blue
- Correlation of oxidative and reductive dye bleaching on TiO₂ photocatalyst films, 119
- Micelles
- Complexation of Mg-tetrabenzoporphyrin with pyridine enhances singlet oxygen generation and affects its partitioning into apolar microenvironments, 7
- Molecular recognition
- Anthracene labeled pyridine amides: A class of prototype PET sensors towards monocarboxylic acid, 40

- Monocarboxylic acid
 Anthracene labeled pyridine amides: A class of prototype PET sensors towards monocarboxylic acid, 40
- Monoolein
 Characterization of mixed DODAB/monoolein aggregates using Nile Red as a solvatochromic and anisotropy fluorescent probe, 32
- Nafion film
 Photoactive component-loaded Nafion film as a platform of hydrogen generation: Alternative utilization of a classical sensitizing system, 112
- Nanocomposites
 Photocatalytic growth of CdS, PbS, and Cu_xS nanoparticles on the nanocrystalline TiO₂ films, 137
- Nile Red
 Characterization of mixed DODAB/monoolein aggregates using Nile Red as a solvatochromic and anisotropy fluorescent probe, 32
- Nitridation
 Visible light-induced photocatalytic oxidation of 4-chlorophenol and dichloroacetate in nitrided Pt-TiO₂ aqueous suspensions, 145
- Nitro-(*E*)-2-azachalcone
 Photochemistry of nitro-substituted (*E*)-2-azachalcones with theoretical calculations and biological activities, 85
- O₂-adsorption
 Physico-chemical, photo-catalytic and O₂-adsorption properties of TiO₂ nanotubes coated with gold nanoparticles, 24
- Oil quality
 Photodegradation of phytosanitary molecules present in virgin olive oil, 1
- Organic solar cell
 Role of a phthalocyanine–fullerene dyad in multilayered organic solar cells, 125
- PAMAM or PPI dendrimer
 Intrinsic luminescence properties of ionic liquid crystals based on PAMAM and PPI dendrimers, 50
- Peroxyl radicals
 Laser flash photolysis of new water-soluble peroxyl radical precursor, 13
- Perylene
 Construction of light-harvesting reverse micelles in nanoscopic dimensions, 56
- Pesticides
 Photosensitizing properties of formulation adjuvants, 186
- PET sensor
 Anthracene labeled pyridine amides: A class of prototype PET sensors towards monocarboxylic acid, 40
- Phosphorescence
 The phosphorescent triplet states of aza-aromatics and their protonated cations in rigid solutions of ethanol and 1-butyl-3-methylimidazolium hexafluorophosphate, 18
- Photocatalysis
 Effect of Fe³⁺ ion doping to TiO₂ on the photocatalytic degradation of Malachite Green dye under UV and vis-irradiation, 64
 Photoactive component-loaded Nafion film as a platform of hydrogen generation: Alternative utilization of a classical sensitizing system, 112
 Photocatalytic growth of CdS, PbS, and Cu_xS nanoparticles on the nanocrystalline TiO₂ films, 137
 Visible light-induced photocatalytic oxidation of 4-chlorophenol and dichloroacetate in nitrided Pt-TiO₂ aqueous suspensions, 145
 Ultra-violet light activated photocatalysis in thin films of the titanium oxynitride, Ti_{3-δ}O₄N, 199
- Photo-catalytic activity
 Physico-chemical, photo-catalytic and O₂-adsorption properties of TiO₂ nanotubes coated with gold nanoparticles, 24
- Photocatalytic degradation
 Correlation of oxidative and reductive dye bleaching on TiO₂ photocatalyst films, 119
- Photochemistry
 Intramolecular interactions and photoinduced electron transfer in isoalloxazine-naphthalene bichromophores, 166
- Photochromic properties
 Photochromic properties of cationic oxazolylfulgimides in hydroxylic media, 161
- Photocyclization
 Solvent-driven adiabatic *trans*-to-*cis* photoisomerization of 4-styrylquinoline, 100
- Photodegradation
 Photodegradation of phytosanitary molecules present in virgin olive oil, 1
 Photosensitizing properties of formulation adjuvants, 186
- Photodimerization
 Photochemistry of nitro-substituted (*E*)-2-azachalcones with theoretical calculations and biological activities, 85
- Photoinduced electron transfer
 Efficient photocleavage of DNA utilizing water soluble riboflavin/naphthaleneacetate substituted fullerene complex, 105
 Role of a phthalocyanine–fullerene dyad in multilayered organic solar cells, 125
- Photoinitiator
 Thioxanthone-benzotriazole: Initiator and stabilizer properties in one component, 81
- Photolysis
 Photodegradation of butylparaben in aqueous solutions by 254 nm irradiation, 131
- Photopolymerization
 A water-soluble two-photon photopolymerization initiation system: Methylated-β-cyclodextrin complex of xanthene dye/aryliodonium salt, 211
- Photosensitization
 Complexation of Mg-tetrabenzoporphyrin with pyridine enhances singlet oxygen generation and affects its partitioning into apolar microenvironments, 7
- Photostabilizer
 Thioxanthone-benzotriazole: Initiator and stabilizer properties in one component, 81
- Photosynthesis
 Photocatalytic growth of CdS, PbS, and Cu_xS nanoparticles on the nanocrystalline TiO₂ films, 137
- Photosynthetic model
 Photoinduced single- and double-electron transfer in a photosynthetic model consisting of one-acceptor with four equally linked donors (D₄-A), 216
- Phthalocyanine
 Photoinduced single- and double-electron transfer in a photosynthetic model consisting of one-acceptor with four equally linked donors (D₄-A), 216
- Phthalocyanine–fullerene dyad
 Role of a phthalocyanine–fullerene dyad in multilayered organic solar cells, 125
- Phytosanitary chemicals
 Photodegradation of phytosanitary molecules present in virgin olive oil, 1
- Polarity
 Characterization of mixed DODAB/monoolein aggregates using Nile Red as a solvatochromic and anisotropy fluorescent probe, 32
- Polycrystalline thin films
 Dependence of photoinduced surface friction force variation on UV intensity and atmosphere in polycrystalline TiO₂ thin films, 155
- Porphyrin
 A density functional theory study on photophysical properties of red light-emitting materials: Meso-substituted porphyrins, 92
- Principal component analysis
 Complexation of Mg-tetrabenzoporphyrin with pyridine enhances singlet oxygen generation and affects its partitioning into apolar microenvironments, 7
- Pt-TiO₂
 Visible light-induced photocatalytic oxidation of 4-chlorophenol and dichloroacetate in nitrided Pt-TiO₂ aqueous suspensions, 145
- Pyridine
 Complexation of Mg-tetrabenzoporphyrin with pyridine enhances singlet oxygen generation and affects its partitioning into apolar microenvironments, 7

- Pyridine amide
 Anthracene labeled pyridine amides: A class of prototype PET sensors towards monocarboxylic acid, 40
- Quantum yield
 Photodegradation of butylparaben in aqueous solutions by 254 nm irradiation, 131
- Quasi-solid state electrolyte
 Sol-gel modified TiO₂ powder films for high performance dye-sensitized solar cells, 192
- Raman
 Ultra-violet light activated photocatalysis in thin films of the titanium oxynitride, Ti₃₋₈O₄N, 199
- Reactive species
 Photosensitizing properties of formulation adjuvants, 186
- Reorganization energy
 A density functional theory study on photophysical properties of red light-emitting materials: Meso-substituted porphyrins, 92
- Resazurin
 Correlation of oxidative and reductive dye bleaching on TiO₂ photocatalyst films, 119
- Riboflavin
 Efficient photocleavage of DNA utilizing water soluble riboflavin/naphthaleneacetate substituted fullerene complex, 105
- Ruthenium bipyridyl sensitizer
 Photoactive component-loaded Nafion film as a platform of hydrogen generation: Alternative utilization of a classical sensitizing system, 112
- Semiconductor nanoparticles
 Photocatalytic growth of CdS, PbS, and Cu_xS nanoparticles on the nanocrystalline TiO₂ films, 137
- Singlet oxygen
 Solvent and central metal effects on the photophysical and photochemical properties of peripherally tetra mercaptopyridine substituted metallophthalocyanines, 204
- Sol-gel
 Sol-gel modified TiO₂ powder films for high performance dye-sensitized solar cells, 192
- Solid films
 Photochromic properties of cationic oxazolyfulgimides in hydroxylic media, 161
- Solvent effect
 Solvent-driven adiabatic *trans*-to-*cis* photoisomerization of 4-styrylquinoline, 100
- Supramolecular complex
 Efficient photocleavage of DNA utilizing water soluble riboflavin/naphthaleneacetate substituted fullerene complex, 105
- Thin film
 Effect of Fe³⁺ ion doping to TiO₂ on the photocatalytic degradation of Malachite Green dye under UV and vis-irradiation, 64
- Thioxanthone
 Thioxanthone-benzotriazole: Initiator and stabilizer properties in one component, 81
- TiO₂
 Effect of Fe³⁺ ion doping to TiO₂ on the photocatalytic degradation of Malachite Green dye under UV and vis-irradiation, 64
 Visible light-induced photocatalytic oxidation of 4-chlorophenol and dichloroacetate in nitrided Pt-TiO₂ aqueous suspensions, 145
- TiO₂ nanotubes
 Physico-chemical, photo-catalytic and O₂-adsorption properties of TiO₂ nanotubes coated with gold nanoparticles, 24
- TiO₂ thick films
 Sol-gel modified TiO₂ powder films for high performance dye-sensitized solar cells, 192
- Titanium dioxide
 Correlation of oxidative and reductive dye bleaching on TiO₂ photocatalyst films, 119
 Photocatalytic growth of CdS, PbS, and Cu_xS nanoparticles on the nanocrystalline TiO₂ films, 137
 Dependence of photoinduced surface friction force variation on UV intensity and atmosphere in polycrystalline TiO₂ thin films, 155
 Ultra-violet light activated photocatalysis in thin films of the titanium oxynitride, Ti₃₋₈O₄N, 199
- Titanium oxynitride
 Ultra-violet light activated photocatalysis in thin films of the titanium oxynitride, Ti₃₋₈O₄N, 199
- Triplet lifetime
 Solvent and central metal effects on the photophysical and photochemical properties of peripherally tetra mercaptopyridine substituted metallophthalocyanines, 204
- Triplet state
 The phosphorescent triplet states of aza-aromatics and their protonated cations in rigid solutions of ethanol and 1-butyl-3-methylimidazolium hexafluorophosphate, 18
- Triplet yields
 Solvent and central metal effects on the photophysical and photochemical properties of peripherally tetra mercaptopyridine substituted metallophthalocyanines, 204
- Visible light
 Photoactive component-loaded Nafion film as a platform of hydrogen generation: Alternative utilization of a classical sensitizing system, 112
 Visible light-induced photocatalytic oxidation of 4-chlorophenol and dichloroacetate in nitrided Pt-TiO₂ aqueous suspensions, 145
- X-ray diffraction
 Ultra-violet light activated photocatalysis in thin films of the titanium oxynitride, Ti₃₋₈O₄N, 199